

Award Number: W81XWH-04-1-0500

TITLE: Structure Optimization of 21,23-Core-Modified Porphyrins Absorbing Long-Wavelength Light as Potential Photosensitizers Against Breast Cancer Cells

PRINCIPAL INVESTIGATOR: Michael R. Detty, Ph.D.

CONTRACTING ORGANIZATION: New York State University  
Amherst, NY 14228-2567

REPORT DATE: April 2007

TYPE OF REPORT: Annual

PREPARED FOR: U.S. Army Medical Research and Materiel Command  
Fort Detrick, Maryland 21702-5012

DISTRIBUTION STATEMENT: Approved for Public Release;  
Distribution Unlimited

The views, opinions and/or findings contained in this report are those of the author(s) and should not be construed as an official Department of the Army position, policy or decision unless so designated by other documentation.

# REPORT DOCUMENTATION PAGE

*Form Approved*  
*OMB No. 0704-0188*

Public reporting burden for this collection of information is estimated to average 1 hour per response, including the time for reviewing instructions, searching existing data sources, gathering and maintaining the data needed, and completing and reviewing this collection of information. Send comments regarding this burden estimate or any other aspect of this collection of information, including suggestions for reducing this burden to Department of Defense, Washington Headquarters Services, Directorate for Information Operations and Reports (0704-0188), 1215 Jefferson Davis Highway, Suite 1204, Arlington, VA 22202-4302. Respondents should be aware that notwithstanding any other provision of law, no person shall be subject to any penalty for failing to comply with a collection of information if it does not display a currently valid OMB control number. **PLEASE DO NOT RETURN YOUR FORM TO THE ABOVE ADDRESS.**

<b>1. REPORT DATE</b> 01-04-2007			<b>2. REPORT TYPE</b> Annual		<b>3. DATES COVERED</b> 1 Apr 2006 – 31 Mar 2007	
<b>4. TITLE AND SUBTITLE</b>  Structure Optimization of 21,23-Core-Modified Porphyrins Absorbing Long-Wavelength Light as Potential Photosensitizers Against Breast Cancer Cells					<b>5a. CONTRACT NUMBER</b>	
					<b>5b. GRANT NUMBER</b> W81XWH-04-1-0500	
					<b>5c. PROGRAM ELEMENT NUMBER</b>	
<b>6. AUTHOR(S)</b>  Michael R. Detty, Ph.D.  Email: <a href="mailto:mdetty@buffalo.edu">mdetty@buffalo.edu</a>					<b>5d. PROJECT NUMBER</b>	
					<b>5e. TASK NUMBER</b>	
					<b>5f. WORK UNIT NUMBER</b>	
<b>7. PERFORMING ORGANIZATION NAME(S) AND ADDRESS(ES)</b>  New York State University Amherst, NY 14228-2567					<b>8. PERFORMING ORGANIZATION REPORT NUMBER</b>	
<b>9. SPONSORING / MONITORING AGENCY NAME(S) AND ADDRESS(ES)</b> U.S. Army Medical Research and Materiel Command Fort Detrick, Maryland 21702-5012					<b>10. SPONSOR/MONITOR'S ACRONYM(S)</b>	
					<b>11. SPONSOR/MONITOR'S REPORT NUMBER(S)</b>	
<b>12. DISTRIBUTION / AVAILABILITY STATEMENT</b> Approved for Public Release; Distribution Unlimited						
<b>13. SUPPLEMENTARY NOTES</b> Original contains colored plates: ALL DTIC reproductions will be in black and white.						
<b>14. ABSTRACT</b> In the first year, we made eighteen new 21,23-core modified porphyrins, determined their photophysical properties, and evaluated the biological properties of them. In the second year, the research focused on 1) analyzing quantitative structure-activity relationships (QSAR) establishing new synthetic methods to prepare eleven new second generation derivatives with novel structures. During the past (third) year, we have evaluated the new derivatives structurally, photophysically, and biologically. The structures of two derivatives were determined unambiguously by x-ray crystallography including the structure of a cis-ABCC meso-substituted derivative and the structure of a cis-AB disubstituted derivative. A series of carboxylic acid-substituted dithiaporphyrins was prepared with different length aliphatic spacers between porphyrin and acid. In a collaborative study with Prof. Benny Ehrenberg at Bar Ilan University in Israel, we found that the efficiency of photooxidizing a membrane-residing singlet oxygen target decreases as the side chains become longer. This has implications for fine-tuning optimal structures for PDT sensitizers. The most promising dithiaporphyrin from in vitro studies is being evaluated in toxicity studies in vivo.						
<b>15. SUBJECT TERMS</b> Photodynamic therapy, breast cancer, core-modified porphyrin, in vitro biological activity						
<b>16. SECURITY CLASSIFICATION OF:</b>				<b>17. LIMITATION OF ABSTRACT</b>	<b>18. NUMBER OF PAGES</b>	<b>19a. NAME OF RESPONSIBLE PERSON</b> USAMRMC
<b>a. REPORT</b> U	<b>b. ABSTRACT</b> U	<b>c. THIS PAGE</b> U	<b>19b. TELEPHONE NUMBER</b> (include area code)			
				UU	21	

## Table of Contents

<b>Cover</b> .....	<b>1</b>
<b>SF 298</b> .....	<b>2</b>
<b>Table of Contents</b> .....	<b>3</b>
<b>Introduction</b> .....	<b>4</b>
<b>Body</b> .....	<b>4</b>
<b>Key Research Accomplishments</b> .....	<b>4</b>
<b>Reportable Outcomes</b> .....	<b>5</b>
<b>Conclusions</b> .....	<b>5</b>
<b>References</b> .....	<b>5</b>
<b>Appendices</b> .....	<b>5</b>

## Introduction

The objectives of this project are two fold: one was to train the former PI, Dr. Youngjae You, as an photodynamic cancer therapy expert in breast cancer research and the other is to perform the research to optimize the structure of 21,23-core-modified porphyrins as potential photosensitizers that are able to absorb long-wavelength light for treating breast cancer. Dr. You has successfully completed his postdoctoral studies and is now a tenure-track assistant professor at the University of South Dakota. His research interests at the University of South Dakota are focused on the synthesis and study of core-modified porphyrins as photosensitizers for the photodynamic therapy of cancer.

In the first year, we made eighteen new 21,23-core modified porphyrins, determined their photophysical properties, and evaluated the biological properties of them. In the second year, the research focused on 1) analyzing quantitative structure-activity relationships (QSAR) establishing new synthetic methods to prepare eleven new second generation derivatives with novel structures. In the second year, the research focused on 1) analyzing quantitative structure-activity relationships (QSAR) establishing new synthetic methods to prepare eleven new second generation derivatives with novel structures.

## Body

Work initiated in the past year is ongoing and will be completed during the additional time afforded by the no cost extension. A series of carboxylic acid-substituted dithiaporphyrins was prepared with different length aliphatic spacers between porphyrin and acid. These 4-(carboxyalkyl)phenyl substituted derivatives had spacers of 1-10 methylene (CH<sub>2</sub>) units. These were prepared via chemistry that was developed in the first two years of this award. In a collaborative study with Prof. Benny Ehrenberg at Bar Ilan University in Israel, we found that the efficiency of photooxidizing a membrane-residing singlet oxygen target decreases as the side chains become longer. We suspect that with these large molecules, when their carboxylates are anchored at the lipid:water interface, the tetrapyrrole is in fact closer to the other, opposite, side of the bilayer. This makes these molecules interesting and different from all the others that have been examined in the literature. Conclusions regarding the location of these materials in the bilayer await the synthesis/purchase of phospholipids that are tagged with fluorophores at their heads.

The structures of two derivatives were determined unambiguously by x-ray crystallography including the structure of a *cis*-ABCC *meso*-substituted derivative and the structure of a *cis*-AB disubstituted derivative. Details of these crystal structures are contained in the appendix in the *J. Porphyrins Phthalocyanines* article. The characterization of the *cis*-ABCC derivative will allow this superior substituent pattern to be isolated unequivocally.

The role of the dithiaporphyrins in inducing apoptosis was determined. This work is summarized in the appendix in the *J. Photochem. Photobiol. B* article. The success of the photosensitizer, I-YY-69, *in vitro* prompted the design of *in vivo* studies to determine 1) its dark toxicity and 2) its efficacy in photodynamic therapy if acceptable toxicity is observed. These studies are ongoing.

## Key Research Accomplishments

**Training:** Dr. You has successfully completed his postdoctoral studies and is now a tenure-track assistant professor at the University of South Dakota. His research interests at the University of South Dakota are focused on the synthesis and study of core-modified porphyrins as photosensitizers for the photodynamic therapy of cancer.

**Research accomplishments:** 1) Synthesis of diverse sets of core-modified porphyrins, 2) determination of physical properties of prepared porphyrins, 3) evaluation of biological effects of the compounds and analysis of structure-activity relationships, 4) elucidating of apoptotic cell death after PDT treatment, and 5) unambiguously determining the structure of two new classes of dithiaporphyrins using x-ray crystallography, and 6) preparing a series of substituted derivatives to probe depth of penetration of the core-modified porphyrins in the lipid bilayer..

## Reportable Outcomes

**Publications:** Part of this report was published in two separate publications included in the appendix at the end of the report;

a) You, Y.; Daniels, T. S.; Dominiak, P. M.; Detty, M. R. "Synthesis, Spectral Data, and Crystal Structure of Two Novel Substitution Patterns in Dithiaporphyrins," *J. Porphyrins Phthalocyanines* **2007**, *11*, 1-8.

b) You, Y.; Gibson, S. L.; Detty, M. R. "Phototoxicity of a Core-modified Porphyrin and Induction of Apoptosis," *J. Photochem. Photobiol. B* **2006**, *85*, 155-162.

**Poster:** Part of Dr. You's work was presented in one poster:

Gannon, Michael K.; Tomblin, Gregory; Donnelly, David J.; Holt, Jason J.; You, Youngjae; Ye, Mao; Nygren, Cara L.; Detty, Michael R. "Characterization of the "R" Binding Site of P-glycoprotein: Using Novel Chalcogenoxanthylum Tetramethylrosamine Analogs for the Stimulation of ATPase Activity," 232<sup>nd</sup> National Meeting of the American Chemical Society, San Francisco, CA (2006).

## Conclusions

Dr. You's postdoctoral studies were completed successfully and he is now employed as an assistant professor in the Department of Chemistry at South Dakota State University. Biological and synthetic studies will be concluded during the coming year with work at both the University at Buffalo and at South Dakota State University.

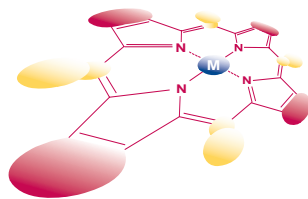
## References

N/A

## Appendices

*J. Porphyrins Phthalocyanines* **2007**, *11*, 1-8.

*J. Photochem. Photobiol. B* **2006**, *85*, 155-162.



## Synthesis, spectral data, and crystal structure of two novel substitution patterns in dithiaporphyrins

Youngjae You<sup>\*a</sup>, Thalia S. Daniels<sup>b</sup>, Paulina M. Dominiak<sup>b</sup> and Michael R. Detty<sup>b◇</sup>

<sup>a</sup> Department of Chemistry & Biochemistry, South Dakota State University, Brookings, South Dakota 57007-0896, USA

<sup>b</sup> Department of Chemistry, University at Buffalo, The State University of New York, Buffalo, New York 14260-3000, USA

Received 1 September 2006

Accepted 2 November 2006

**ABSTRACT:** The syntheses, characterizations and crystal structures of 5-(4-*tert*-butylphenyl)-15,20-diphenyl-10-(4-methoxy)phenyl-21,23-dithiaporphyrin (**1b**) and 2,3-dimethoxy-10,15-diphenyl-21,23-dithiaporphyrin (**2**) are described. The cyclization of 2-[1-(4-methoxyphenyl)-1-pyrrolo-methyl]-5-(1-phenyl-1-pyrrolo-methyl)thiophene and 2-[1-(4-*t*-butylphenyl)-1-hydroxymethyl]-5-(1-phenyl-1-hydroxymethyl)thiophene gave predominantly the *cis*-regioisomer, which was characterized by X-ray crystallography. Copyright © 2007 Society of Porphyrins & Phthalocyanines.

**KEYWORDS:** core-modified porphyrin, synthesis, X-ray crystal structure, spectral data.

### INTRODUCTION

Porphyrin derivatives have been developed or are under development as photosensitizers for photodynamic therapy due to the favorable photophysical characteristics of porphyrins: absorbing light of 630 nm and generating singlet oxygen effectively [1, 2]. However, photosensitizers in deeper tissues can only be activated by light that penetrates, which is preferably in the 650-800 nm range [3]. The substitution of the core nitrogen atom(s) of natural porphyrins with heavy atoms such as S, Se, and Te provides a red-shift in their absorption spectra [4-7]. The 21,23-dithiaporphyrin core, especially, is an excellent pharmacophore for good photosensitizers, absorbing light of about 700 nm as well as generating singlet oxygen effectively [5]. Some dithiaporphyrins having two carboxylic acids expressed sub-micromolar phototoxicity *in vitro* when activated with minimal light 5 J.cm<sup>-2</sup> of filtered, 350-750 nm broad band light [8-10].

While the core atoms of porphyrins affect their photophysical properties, the structure and placement of *meso* substituents might influence the binding with biological components such as membranes, enzymes, receptors, and lipoproteins. The binding with possible molecular targets might subsequently determine the biological efficiency of the porphyrins as photosensitizers. In our studies of structure-activity relationships between core-modified porphyrins and phototoxicity, we clearly observed the effects of the size and the symmetry of the placement of substituents at *meso*-aryl groups on their phototoxicity [9, 10].

Syntheses of 21,23 core-modified porphyrins were pioneered by Ulman *et al.* [11-15]. More recently, Lee's group published a [3 + 1] cyclization method to prepare various types of core-modified porphyrins with [A<sub>2</sub>B<sub>2</sub>]-substitution patterns [16, 17] and Chandrashekar's group developed a convenient method for the synthesis of expanded core-modified porphyrins [18-20]. However, studies of structure-activity relationships directed toward phototoxicity in core-modified porphyrins are limited by the available synthetic methods for their preparation. In particular, few synthetic methods are available for the

◇SPP full member in good standing

\*Correspondence to: Youngjae You, email: youngjae.you@sdstate.edu, fax: +1 605-688-6364

synthesis of dithiaporphyrins with more diverse substituents at the *meso*-positions. This is especially the case of the 21,23-dithiaporphyrins of which the synthesis and characterization of *cis*-[ABC<sub>2</sub>]- and *trans*-[ABC<sub>2</sub>]-substitution patterns in the *meso*-substituents have not been described [8], and derivatives with unsubstituted *meso*-substituents are also very scarce [21, 22]. Herein, we report the synthesis, characterization, and X-ray crystal structures of two novel dithiaporphyrins: 5-(4-*tert*-butylphenyl)-15,20-diphenyl-10-(4-methoxyphenyl)-21,23-dithiaporphyrin **1b** (a *cis*-[ABC<sub>2</sub>] *meso*-substituent pattern) and 2,3-dimethoxy-10,15-diphenyl-21,23-dithiaporphyrin **2** (unsubstituted *meso* substituents).

## RESULTS AND DISCUSSION

### Synthesis and characterization

The facile [3 + 1] type condensation reaction was adopted in the cyclization for the dithiaporphyrins, **1b** and **2**. The precursors **4**, **5**, and **8** were prepared from the aldehydes and thiophene by methods described in our previous study [9]. The yield of the condensation reaction to give compound **7** was poor (27%) relative to the 75% yield for the condensation reaction to give compound **4**. From the cyclization reaction of **4** and **5**, we expected to get two regioisomeric dithiaporphyrins, *trans* and *cis*-forms. Indeed two spots, presumably of two isomers, were observed by thin layer chromatography (TLC). The upper spot was isolated in yields too low to allow characterization.

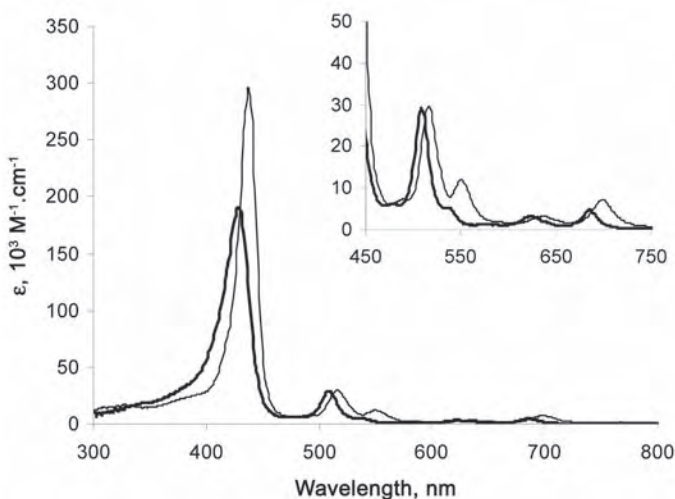


**Fig. 1.** Electronic absorption spectra of **1b** (thin line) and **2** (thick line)

**Table 1.** Wavelengths and excitation coefficients of electronic absorption spectra of compounds **1b**, **2**, and **9**

**9**

<b>9<sup>a</sup></b>		<b>1b</b>		<b>2</b>	
$\lambda_{\max}^b$	$\epsilon^c$	$\lambda_{\max}$	$\epsilon$	$\lambda_{\max}$	$\epsilon$
435	297.5	437	279.3	428	175.5
515	29.6	516	26.6	509	25.6
548	7.3	550	12.4	536	4.0
635	2.2	635	2.0	622	2.4
699	4.6	699	6.0	685	3.8

<sup>a</sup> **9**: 5,10,15,20-tetraphenyl-21,23-dithiaporphyrin, the data of compound **9** were adopted from the reference 15; <sup>b</sup> nm; <sup>c</sup>  $10^3 \text{ M}^{-1} \cdot \text{cm}^{-1}$ ; the solvents:  $\text{CH}_2\text{Cl}_2$  for compounds **1b** and **2** and  $\text{CHCl}_3$  for compound **9**.

However, the second product, *cis*-form (**1b**), was successfully isolated and characterized in 18% yield. Spectroscopic data (<sup>1</sup>H, <sup>13</sup>C NMR, and high mass) were consistent with the assigned structure, which was confirmed by X-ray crystal data. On the other hand, the cyclization to give **2** gives a single isomer in 18%. The two *meso*-hydrogens of dithiaporphyrin **2** gave a characteristic peak in the <sup>1</sup>H NMR spectrum at 10.73 ppm while high resolution MS mass data were consistent with the expected molecular formula. The structure of **2** was confirmed by X-ray crystal data.

The UV-vis spectra of compounds **1b**, **2**, and **9** shown in Fig. 1 are typical core-modified porphyrinic spectra with four weak Q-bands and one strong Soret band in the visible range. For the asymmetric dithiaporphyrin **1b**, the properties of the bands,  $\lambda_{\max}$ 's and  $\epsilon$ 's, are very close to those of the symmetric 5,10,15,20-tetraphenyl-21,23-dithiaporphyrin (**9**) (Table 1) [15]. On the other hand, the electronic absorptions in the spectrum of compound **2** are quite different from those in the spectra of **9** and **1b** (Fig. 1). The Soret band is blue-shifted, by about 7 and 9 nm, and its excitation coefficient is smaller,  $1.76 \times 10^5 \text{ M}^{-1} \cdot \text{cm}^{-1}$ , than those of compounds **9** and **1b**. While all four Q bands of **2** are blue-shifted, the effects on extinction coefficients are more pronounced

in bands I and III,  $1.24$  and  $7.3 \times 10^4 \text{ M}^{-1} \cdot \text{cm}^{-1}$  vs  $4 \times 10^3 \text{ M}^{-1} \cdot \text{cm}^{-1}$  for band III and  $6$  and  $4.6 \times 10^3 \text{ M}^{-1} \cdot \text{cm}^{-1}$  vs  $3.8 \times 10^3 \text{ M}^{-1} \cdot \text{cm}^{-1}$  for band I. These data demonstrate that the number of aryl groups at the *meso* positions affects the electronic spectra more (**9** vs **2**) than the molecular symmetry of tetra-aryl dithiaporphyrin (**9** vs **1b**). In other words, while structural variations between **2** and **9** reside directly on the dithiaporphyrin ring, the structural differences between **1b** and **9** are at the *para* positions of meso aryl rings.

### X-ray structures of **1b** and **2**

The identification of the major isomer isolated from the synthesis shown in Scheme 1 was obtained *via* X-ray crystallographic analysis. Other spectroscopic methods would not be able to assign unequivocally the correct regiochemistry to the porphyrin molecule. The black and planar single crystals of **1b** were obtained by direct solvent diffusion of *n*-hexane into a saturated solution in dichloromethane over a 3-week period in a cold room. The dithiaporphyrin core of the molecule is almost planar ( $0.073 \text{ \AA}$  of mean deviation from the plane, Fig. 2). The phenyl rings are rotated out of the core plane ( $55^\circ$ ,  $62^\circ$ ,  $64^\circ$  and  $79^\circ$ ). The N1...N2 distance is elongated ( $4.614$

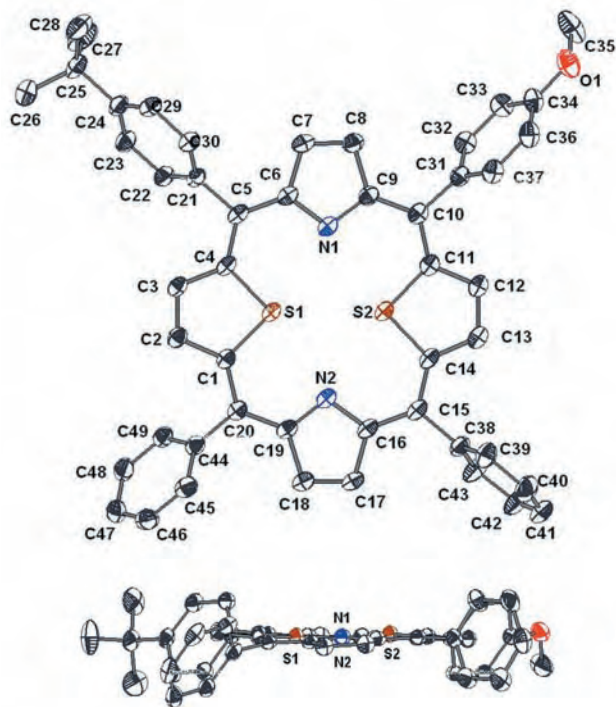


**Fig. 2.** Structure of compound **1b** viewed (a) from the top and (b) from the side with hydrogen atoms omitted for clarity. Displacement ellipsoids are drawn at the 50% probability level

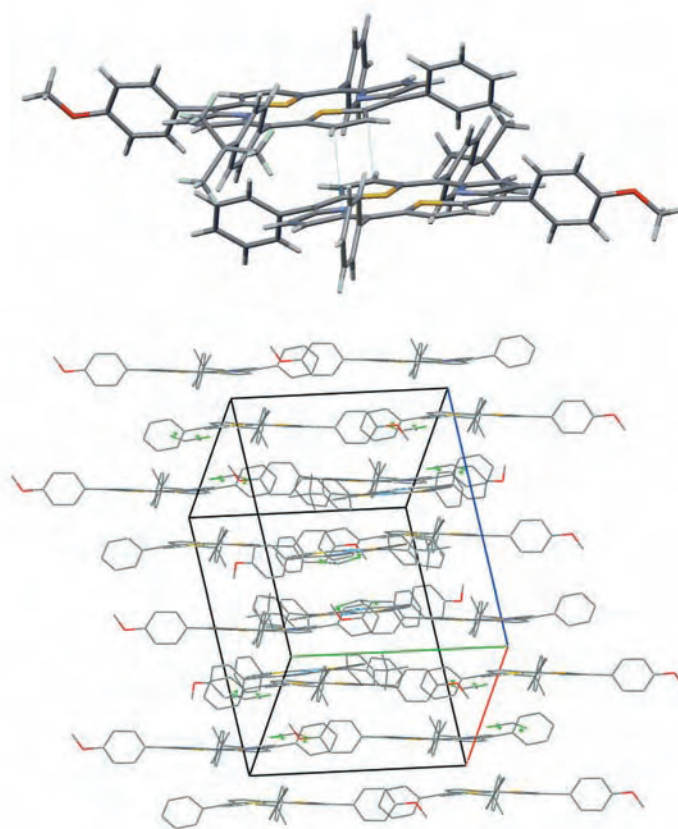


**Fig. 3.** The  $\pi \dots \pi$  interactions between the two closest molecules in the crystal lattice and the molecular packing diagram of compound **1b**. Unit cell axis *a* shown in red, *b* in green and *c* in blue

$\text{\AA}$ ) compared with a natural four nitrogenic porphyrin ( $4.042 \text{ \AA}$ ) [23] to accommodate the large S atoms. Two molecules form a dimer in the crystal lattice mainly *via* C–H... $\pi$  and  $\pi \dots \pi$  interactions with the distance between dithiaporphyrin planes equal to  $3.63 \text{ \AA}$  (Fig. 3). The interplanar distance is slightly longer than the typical separation for aggregated porphyrins which is  $3.4$ – $3.6 \text{ \AA}$  [24]. The centers of the molecules are offset by  $5.55 \text{ \AA}$  which again is outside the usual limits ( $3$ – $4 \text{ \AA}$ ) for  $\pi \dots \pi$  interacting porphyrins. This very weak  $\pi \dots \pi$  face-to-face interaction is supported by C–H... $\pi$  face-to-edge interactions (C(45)–H(31)...N(1) distance equal to  $3.345 \text{ \AA}$ ) to form a dimer. Two dichloromethane molecules of solvation, one for each porphyrin **1b**, were omitted for clarity in the figure.

The single crystals of compound **2** were also grown by direct solvent diffusion of *n*-hexane into a saturated solution in dichloromethane over a week. The black, planar crystals were characterized by X-ray crystallography. The core of the dithiaporphyrin is planar ( $0.035 \text{ \AA}$  of mean devia-

tion from the plane, Fig. 4). The phenyl rings and one of the methoxy groups are nearly perpendicular to the core (81°, 64° and 77°, respectively) whereas the second methoxy group is almost in the plane of the core. The N1...N2 distance is also increased (4.584 Å) compared to four nitrogenic porphyrin (4.042 Å) [23]. Two molecules form a dimer in the crystal lattice mainly *via*  $\pi$ ... $\pi$  interactions (Fig. 5) with the distance between dithiaporphyrin planes equal to 3.41 Å. This intraplanar distance together with 3.55 Å offset is typical for strong cofacial  $\pi$ ... $\pi$  interaction observed in porphyrins [24].

The crystal structures of compounds **1b** and **2** show different dimerization patterns. The interaction between two molecules of **2** seems to be stronger and the distance between two molecules is shorter, 3.41 Å relative to the dimers of **1b**, 3.63 Å. For **2**, the dimeric molecules are more overlapped due to reduced steric interactions of the *meso*-phenyl groups on one molecule with the unsubstituted *meso*-positions of the other. Interestingly, the dimers of **1b** are organized in parallel sheets while the dimers of **2** show perpendicular stacking.

There are three other structures of free base 21,23-dithiaporphyrin derivatives deposited in the Cambridge Structural Database: [25] 5,10,15,20-tetrakis(2-thienyl)-21,23-dithiaporphyrin [26], 21,23-dithiate-traphenylporphyrin [27], and 2,3,12,13-tetrabutoxy-5,10,15,20-tetraphenyl-21,23-dithiaporphyrin [28] (Refcodes: BEHGUR, DTHTPP02 and XUJZUK, respectively). Porphyrin cores overlap only in the

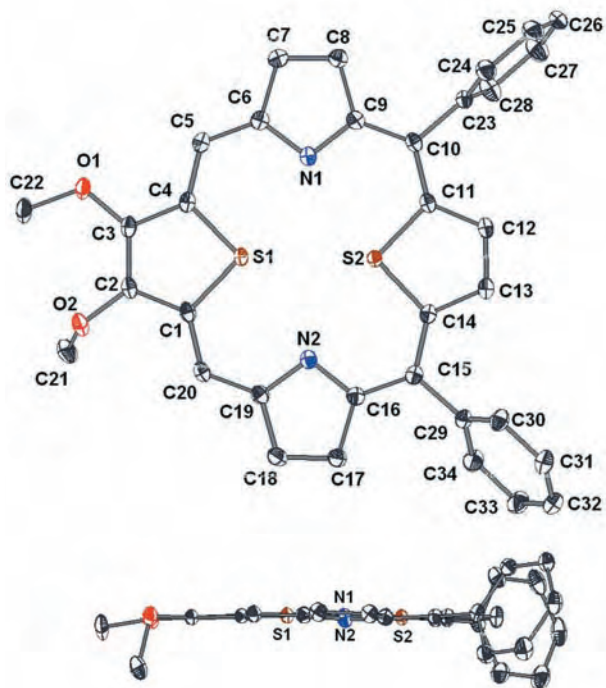


**Fig. 4.** Structure of compound **2** viewed (a) from the top and (b) from the side with hydrogen atoms omitted for clarity. Displacement ellipsoids are drawn at the 50% probability level

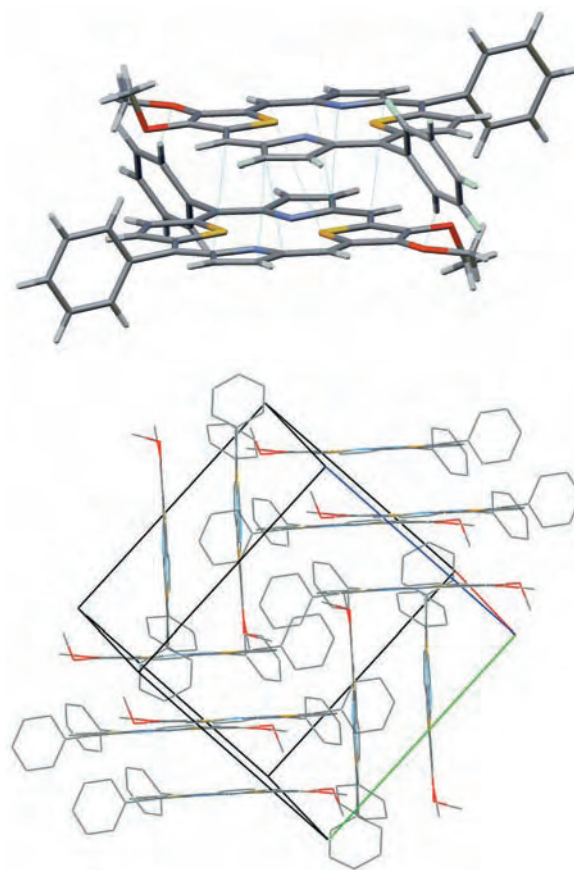


**Fig. 5.** The  $\pi$ ... $\pi$  interactions between the two closest molecules in the crystal lattice and the molecular packing diagram of compound **2**. Unit cell axis *a* shown in red, *b* in green and *c* in blue

first structure (BEHGUR) with a fairly large interplanar distance (3.71 Å) and offset (4.83 Å). However, they do not form isolated dimers but rather form a single strand with molecules placed equidistantly from each other. In the remaining structures, distances between the two closest parallel porphyrin cores are much bigger (4.49 and 4.66 Å in DTHTPP02 and XUJZUK, respectively) and the parallel shift is larger than the size of the porphyrine core (10.85 and 7.24 Å for DTHTPP02 and XUJZUK, respectively).

## EXPERIMENTAL

### Materials

Solvents and reagents were used as received from Sigma-Aldrich Chemical Co. (St. Louis, MO) unless otherwise noted. Concentration *in vacuo* was performed on a Buchi rotary evaporator. NMR spectra were recorded at 23 °C on a Varian Gemini-300,

Inova 400, or Inova 500 instrument with residual solvent signal as the internal standard:  $\text{CDCl}_3$  ( $\delta$  7.26 for proton,  $\delta$  77.16 for carbon) or  $\text{CD}_2\text{Cl}_2$  ( $\delta$  5.32 for proton,  $\delta$  54.00 for carbon). Infrared spectra were recorded on a Perkin-Elmer FT-IR instrument. UV-visible near-IR spectra were recorded on a Perkin-Elmer Lambda 12 spectrophotometer. ESI mass spectrometries were conducted by the Instrument Center of the Department of Chemistry at the University at Buffalo.

### Synthesis

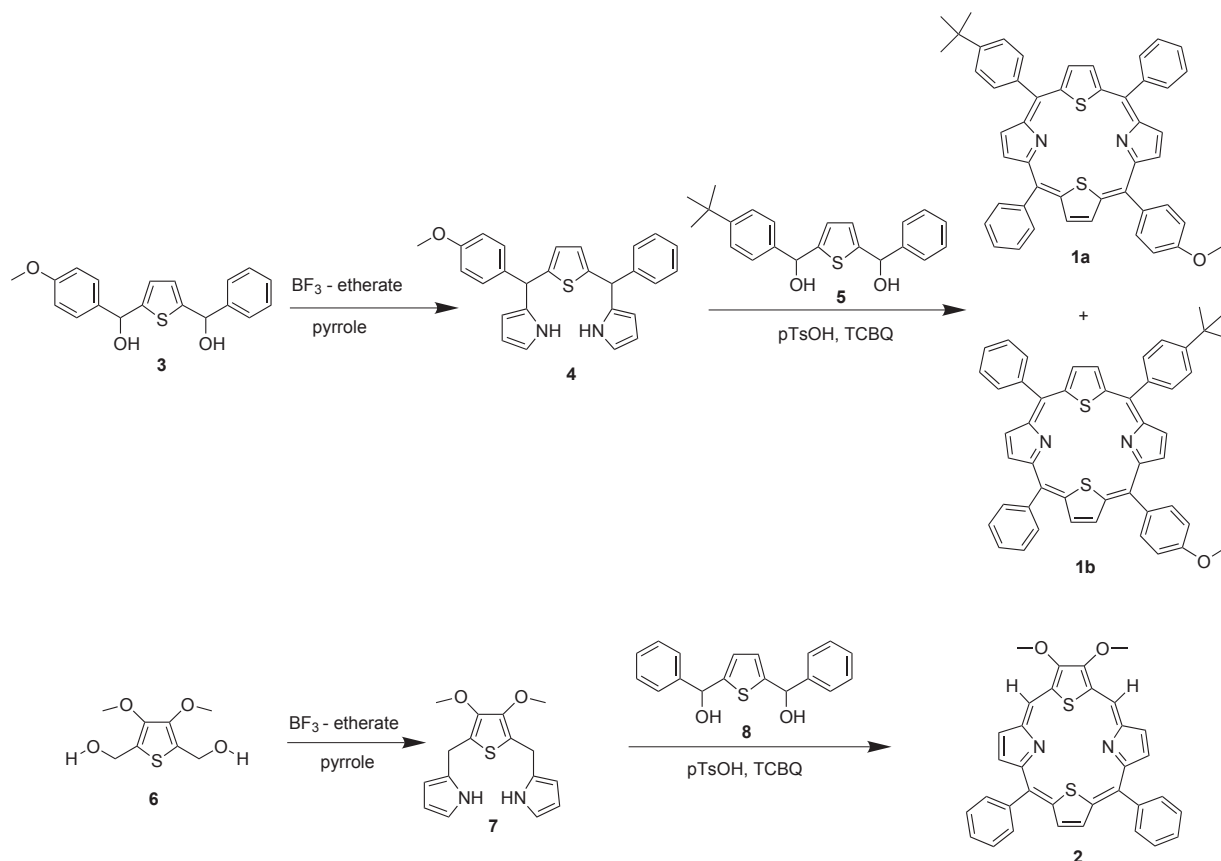
Compound **6** was prepared as described in the literature [22, 29] and compounds **3**, **5**, **8** were prepared by methods described in our earlier work [8, 9].

**Synthesis of 2-[1-(4-methoxyphenyl)-1-pyrrolo-methyl]-5-(1-phenyl-1-pyrrolo-methyl)thiophene 4.** Compound **3** (3.64 g, 0.011 mol) was dissolved in excess pyrrole (23 mL, 0.33 mol) and stirred at ambient temperature for 2 h. Boron trifluoride etherate (0.14 mL, 0.0011 mol) was added and the mixture stirred for another 2.5 h at ambient temperature. The reaction was stopped by the addition of 20 mL of dichloromethane followed by 40% NaOH (15 mL). The organic phase was separated and washed with

distilled water ( $3 \times 15$  mL) and brine ( $1 \times 15$  mL), dried over  $\text{MgSO}_4$  and concentrated. Excess pyrrole was removed *via* vacuum distillation at  $80^\circ\text{C}$  for 2 h. The brown oil was then purified by column chromatography on silica gel eluted with a 5:1 mixture of hexanes/ethyl acetate to give 3.20 g (68%) of **4** as a light brown oil.  $^1\text{H NMR}$  (500 MHz,  $\text{CDCl}_3$ ):  $\delta_{\text{H}}$ , ppm 3.79 (s, 3 H), 5.52 (s, 1 H), 5.56 (s, 1 H), 5.91 (s, 2 H), 6.14 (s, 2 H), 6.61 (s, 2 H), 6.69 (s, 2 H), 6.84 (d, 2 H,  $J = 8.8$  Hz), 7.15 (d, 2 H,  $J = 8.4$  Hz), 7.23–7.38 (m, 5 H), 7.89 (s, 2H).  $^{13}\text{C NMR}$  (75 MHz,  $\text{CDCl}_3$ ):  $\delta_{\text{C}}$ , ppm 45.7, 46.6, 55.8, 107.9, 108.0, 108.7, 108.8, 114.5, 117.7, 118.2, 125.7, 125.9, 127.6, 128.9, 129.1, 129.9, 133.6, 133.9, 135.4, 143.2, 146.2, 146.9, 159.1. LRMS (ESI):  $m/z$  425.2. Calcd. for  $\text{C}_{27}\text{H}_{24}\text{N}_2\text{OS} + \text{H}^+$ : 425.2.

**Synthesis of 3,4-dimethoxy-2,5-bis[(1-pyrrolo-methyl)]-thiophene 7.** Compound **7** was prepared from compound **1** by methods similar to those used for the preparation of compound **4**. Yield 27%.  $^1\text{H NMR}$  (400 MHz,  $\text{CDCl}_3$ ):  $\delta_{\text{H}}$ , ppm 3.85 (6H, s), 3.93 (4H, s), 5.99 (2H, s), 6.10 (2H, s), 6.67 (2H, s), 8.32 (2H, br s). LRMS (ESI):  $m/z$  303.0. Anal. calcd. for  $\text{C}_{16}\text{H}_{18}\text{N}_2\text{O}_2\text{S} + \text{H}^+$ : 303.1.

**Synthesis of 5-(4-*tert*-butylphenyl)-15,20-diphenyl-10-(4-methoxy)phenyl-21,23-dithiaporphyrin**



**Scheme 1.** Synthetic schemes for 5-(4-*tert*-butylphenyl)-15,20-diphenyl-10-(4-methoxy)phenyl-21,23-dithiaporphyrin (**1b**) and 2,3-dimethoxy-10,15-diphenyl-21,23-dithiaporphyrin (**2**)

**1b**. Compound **5** (1.45 g, 0.0041 mol), **4** (1.75 g, 0.0041 mol), and *p*-toluenesulfonic acid (0.78 g, 0.0041 mol) were dissolved in 510 mL of dichloromethane. The reaction vessel was covered completely with foil and stirred in the dark at ambient temperature for 0.5 h. Tetrachlorobenzoquinone (TCBQ) (4.05 g, 0.017 mol) was added and the solution was heated at reflux for 1.5 h. The reaction mixture was cooled to ambient temperature, filtered, and concentrated. The crude product was purified several times *via* column chromatography on basic alumina eluted with a 1:1 mixture of dichloromethane/hexanes. Porphyrin **1b** was isolated as the second red band. The product was washed with minimal acetone several times to retrieve 0.549 g (18%) of **1b** as a purple solid. mp >300 °C. <sup>1</sup>H NMR (500 MHz, CDCl<sub>3</sub>): δ<sub>H</sub>, ppm 1.61 (s, 9H), 4.10 (s, 3H), 7.39 (d, 2H, *J* = 8.5 Hz), 7.82–7.90 (m, 8H), 8.17–8.22 (m, 4H), 8.26 (d, 4H, *J* = 6.0 Hz), 8.70 (d, 2H, *J* = 3.2 Hz), 8.73 (d, 2H, *J* = 3.2 Hz), 9.71 (d, 2H, *J* = 5.0 Hz), 9.76 (d, 1H, *J* = 5.0 Hz), 9.77 (d, 1H, *J* = 5.5 Hz). <sup>13</sup>C NMR (75 MHz, CDCl<sub>3</sub>): δ<sub>C</sub>, ppm 32.2, 35.5, 56.1, 113.6, 125.0, 127.9, 128.5, 134.3, 134.4, 134.5, 134.6, 134.7, 134.7, 135.0, 135.2, 136.0, 136.2, 138.8, 141.9, 148.4, 148.4, 151.5, 156.9, 157.2, 160.3. HRMS (ESI): *m/z* 735.2693. Anal. calcd. for C<sub>49</sub>H<sub>38</sub>ON<sub>2</sub><sup>32</sup>S<sub>2</sub> + H<sup>+</sup>: 735.2710.

**Synthesis of 2,3-dimethoxy-10,15-diphenyl-21,23-dithiaporphyrin (2)**. Dithiaporphyrin **2** was prepared from compounds **7** and **8** by methods similar to those used for the preparation of compound **1b**. Yield 18%, mp >300 °C. <sup>1</sup>H NMR (400 MHz, CD<sub>2</sub>Cl<sub>2</sub>): δ<sub>H</sub>, ppm 4.95 (6H, s), 7.88 (6H, s), 8.29 (4H, d, *J* = 4.0 Hz), 8.82 (2H, d, *J* = 3.6 Hz), 9.10 (2H, d, *J* = 3.6 Hz), 9.75 (2H, s), 10.73 (2H, s). <sup>13</sup>C NMR (75 MHz, CD<sub>2</sub>Cl<sub>2</sub>): δ<sub>C</sub>, ppm 63.2, 113.7, 127.6, 128.3, 134.1, 134.3, 134.5, 135.1, 135.3, 136.6, 141.0, 147.6, 151.0, 155.3, 155.9. HRMS (ESI): *m/z* 557.1352. Anal. calcd. for C<sub>34</sub>H<sub>24</sub>O<sub>2</sub>N<sub>2</sub><sup>32</sup>S<sub>2</sub> + H<sup>+</sup>: 557.1352).

#### X-ray data collection and refinement

X-ray diffraction data on **1b** and **2** were collected at 90(1)K using a Brüker SMART APEX2 CCD diffractometer installed at a rotating anode source (MoK $\alpha$  radiation,  $\lambda$  = 0.71073 Å), and equipped with an Oxford Cryosystems nitrogen gas-flow apparatus. The data were collected by the rotation method with 0.5° (0.3° for compound **2**) frame-width ( $\omega$  scan) and 35 (20 for compound **2**) s exposure time per frame. Four sets of data (360 (600 for compound **2**) frames in each set) were

collected, nominally covering complete reciprocal space. The data were integrated, scaled, sorted and averaged using the SMART software package [30]. The structure was solved by Direct methods using SHELXTL NT Version 6.14 [31]. The structure was refined by full-matrix least squares against F<sup>2</sup>. Non-hydrogen atoms were refined anisotropically. Positions of hydrogen atoms were found by difference electron density Fourier synthesis. The CH<sub>3</sub> hydrogens were treated as part of idealized CH<sub>3</sub> groups with U<sub>iso</sub> = 1.5U<sub>eq</sub>, while the remainder of the hydrogen atoms were refined with the “riding” model with U<sub>iso</sub> = 1.2U<sub>eq</sub>. Structure refinement data are given in Table 2. Atomic coordinates, anisotropic displacement parameters, bond lengths and angles are given in the supporting information section.

## CONCLUSION

Two novel dithiaporphyrins substitution patterns were incorporated in the synthesis and characterization of compounds **1b** and **2**. The structures of **1b** and **2** were unambiguously confirmed by X-ray crystallography and the major isomer produced in the preparation of the *meso*-[ABC<sub>2</sub>] dithiaporphyrins **1** was the *cis*-regioisomer **1b**. The first

**Table 2.** Crystallographic data for **1b** and **2**

Compound	<b>1b</b>	<b>2</b>
Formula	C <sub>49</sub> H <sub>38</sub> N <sub>2</sub> O <sub>2</sub> S <sub>2</sub> ·CH <sub>2</sub> Cl <sub>2</sub>	C <sub>34</sub> H <sub>24</sub> N <sub>2</sub> O <sub>2</sub> S <sub>2</sub>
M <sub>r</sub> , g·mol <sup>-1</sup>	819.86	556.67
T [K]	90(1)	90(1)
Space group	P2 <sub>1</sub> /c	P2 <sub>1</sub> /n
<i>a</i> , Å	13.0893(3)	14.8335(6)
<i>b</i> , Å	15.2550(4)	12.8034(5)
<i>c</i> , Å	20.4068(5)	14.9590(6)
$\beta$ , °	95.7150(10)	112.8560(10)
<i>V</i> , Å <sup>3</sup>	4054.52(17)	2617.94(18)
<i>Z</i>	4	4
$\rho_{\text{calc}}$ , g·cm <sup>-3</sup>	1.343	1.412
$\mu$ , mm <sup>-1</sup>	0.305	0.241
Reflections measured	63002	39987
Unique reflections (R <sub>int</sub> )	10082 (0.028)	6490 (0.022)
Parameters refined	531	363
R [ <i>I</i> > 2 $\sigma$ ( <i>I</i> )]	0.055	0.031
wR <sub>2</sub> [ <i>I</i> > 2 $\sigma$ ( <i>I</i> )]	0.15	0.079
G.O.F.	1.03	1.03

dithiaporphyrin bearing two unsubstituted *meso*-positions was also prepared and characterized. The aromatic groups at the *meso* positions influenced the electronic absorption spectra both in the wavelength and the oscillator strength of the absorption. With these structurally novel dithiaporphyrins in hand, the synthesis of other derivatives will now be facilitated and these substitution patterns will be evaluated for their utility as photosensitizers for photodynamic therapy.

### Supporting information

Crystallographic data of compound **1b** and **2** including atomic coordinations, equivalent isotropic displacement parameters, anisotropic displacement parameters, and bond lengths and angles are available. Crystallographic data have been deposited at the CCDC, 12 Union Road, Cambridge CB2 1EZ, UK and copies can be obtained on request, free of charge, by quoting the publication citation and the deposition numbers 615619 for **1b** and 615620 for **2**.

### Acknowledgements

This research was supported by the Department of Defense [Breast Cancer Research Program] under award number (W81XWH-04-1-0500). Views and opinions of, and endorsements by the author(s) do not reflect those of the US Army or the Department of Defense.

### REFERENCES

1. Nyman ES and Hynninen PH. *J. Photochem. Photobiol. B* 2004; **73**: 1-28.
2. Pandey RK and Zheng G. In *The Porphyrin Handbook* Vol. 6, Kadish KM, Smith KM, Guillard R. (Eds.) Academic Press: San Diego, Calif, 2000; pp 157-230.
3. Detty MR. *Expert Opin. Ther. Pat.* 2001; **11**: 1849-1860.
4. Stilts CE, Nelen MI, Hilmey DG, Davies SR, Gollnick SO, Oseroff AR, Gibson SL, Hilf R and Detty MR. *J. Med. Chem.* 2000; **43**: 2403-2410.
5. Hilmey DG, Abe M, Nelen MI, Stilts CE, Baker GA, Baker SN, Bright FV, Davies SR, Gollnick SO, Oseroff AR, Gibson SL, Hilf R and Detty MR. *J. Med. Chem.* 2002; **45**: 449-461.
6. Abe M, Hilmey DG, Stilts CE, Sukumaran DK and Detty MR. *Organometallics* 2001; **21**: 2986-2992.
7. Abe M, Detty MR, Gerlits OO and Sukumaran DK. *Organometallics* 2004; **23**: 4513-4518.
8. You Y, Gibson SL, Hilf R, Davies SR, Oseroff AR, Roy I, Ohulchanskyy TY, Bergey EJ and Detty MR. *J. Med. Chem.* 2003; **46**: 3734-3747.
9. You Y, Gibson SL, Hilf R, Ohulchanskyy TY and Detty MR. *Bioorg. Med. Chem.* 2005; **13**: 2235-2251.
10. You Y, Gibson SL and Detty MR. *Bioorg. Med. Chem.* 2005; **13**: 5968-5980.
11. Ulman A, Manassen J, Frolow F and Rabinovich D. *J. Am. Chem. Soc.* 1979; **101**: 7055-7059.
12. Ulman A and Manassen J. *J. Chem. Soc., Perkin Trans. I* 1979: 1066-1069.
13. Ulman A, Manassen J, Frolow F and Rabinovich D. *Tetrahedron Lett.* 1978: 167-170.
14. Ulman A, Manassen J, Frolow F and Rabinovich D. *Tetrahedron Lett.* 1978: 1885-1886.
15. Ulman A and Manassen J. *J. Am. Chem. Soc.* 1975; **97**: 6540-6544.
16. Lee C-H, Park J-Y and Kim H-J. *Bull. Korean Chem. Soc.* 2000; **21**: 97-100.
17. Heo P-Y, Shin K and Lee C-H. *Tetrahedron Lett.* 1996; **37**: 197-200.
18. Narayanan SJ, Sridevi B, Chandrashekar TK, Vij A and Roy R. *J. Am. Chem. Soc.* 1999; **121**: 9053-9068.
19. Srinivasan A, Mahajan S, Pushpan SK, Ravikumar M and Chandrashekar TK. *Tetrahedron Lett.* 1998; **39**: 1961-1964.
20. Pushpan SK, Narayanan JS, Srinivasan A, Mahajan S, Chandrashekar TK and Roy R. *Tetrahedron Lett.* 1998; **39**: 9249-9252.
21. Punidha S, Agarwal N, Burai R and Ravikanth M. *Eur. J. Org. Chem.* 2004: 2223-2230.
22. Agarwal N, Hung C-H and Ravikanth M. *Eur. J. Org. Chem.* 2003: 3730-3734.
23. Kano K, Fukuda K, Wakami H, Nishiyabu R and Pasternack RF. *J. Am. Chem. Soc.* 2000; **122**: 7494-7502.
24. Hunter CA and Sanders JKM. *J. Am. Chem. Soc.* 1990; **112**: 5525-5534.
25. Allen Frank H. *Acta Crystallogr., Sect. B: Struct. Sci.* 2002; **58**: 380-388.
26. Gupta I, Hung CH and Ravikanth M. *Eur. J. Org. Chem.* 2003: 4392-4400.
27. Latos-Grazynski L, Lisowski J, Szterenber L, Olmstead MM and Balch AL. *J. Org. Chem.* 1991; **56**: 4043-4045.
28. Agarwal N, Mishra SP, Kumar A, Hung CH and Ravikanth M. *Chem. Commun. (Cambridge, U. K.)* 2002: 2642-2643.
29. Aitken RA and Garnett AN. *J. Chem. Soc., Perkin Trans. I* 2000: 3020-3021.
30. In *APEX2 and SAINT-Plus, Area detector control and integration software, Ver. 1.0-27*

Bruker Analytical X ray Systems: Madison, Wisconsin, USA, 2004.

31. In *SHELXTL, An integrated system for solving, refining and displaying crystal structures from*

*diffraction data, Ver. 6.14* Bruker Analytical X-ray Systems: Madison, Wisconsin, USA, 2003.



# Phototoxicity of a core-modified porphyrin and induction of apoptosis

Youngjae You <sup>a,\*</sup>, Scott L. Gibson <sup>b</sup>, Michael R. Detty <sup>a</sup>

<sup>a</sup> Department of Chemistry, University at Buffalo, The State University of New York, Buffalo, NY 14260-3000, United States

<sup>b</sup> Department of Biochemistry and Biophysics, University of Rochester Medical Center, 601 Elmwood Avenue, Box 607, Rochester, NY 14642, United States

Received 4 April 2006; received in revised form 20 June 2006; accepted 3 July 2006

## Abstract

A core-modified porphyrin, 5-phenyl-10,15-bis(carboxylatomethoxyphenyl)-20-(2-thienyl)-21,23-dithiaporphyrin (**IY69**) was studied in vitro for photodynamic activity under a variety of experimental protocols. Variables included the cell line (the rodent mammary tumor cell line R3230AC or the human breast cancer cell line MCF-7), light fluence, time of exposure of the cell cultures to **IY69**, and the time post-irradiation for cell counting. The length of time cell cultures were exposed to **IY69** impacted cellular accumulation and cellular localization, phototoxicity, and the apparent mode of cell death – apoptosis vs. necrosis.

© 2006 Elsevier B.V. All rights reserved.

**Keywords:** Core-modified porphyrin; Breast cancer; Photodynamic therapy; Apoptosis

## 1. Introduction

Photodynamic therapy (PDT) is a promising strategy for the treatment of cancer [1–4]. PDT has regulatory approval from numerous agencies in the US, Canada, Japan, Great Britain, and Europe for treating a variety of human malignancies [1–5]. PDT requires three components: a photosensitizer, oxygen, and light. PDT is made more effective by increasing the selectivity of the photosensitizer for targeted tissues and by the selective delivery of light via fiber optics. Singlet oxygen is the primary phototoxic species generated by most photosensitizers upon irradiation and the damage induced by singlet oxygen results first in injury to cellular function and structure, and ultimately in cell death and regression of lesions [6]. One major focus of PDT research has been directed towards synthesizing more effective photosensitizers [7]. The criteria for an effective photosensitizer are that it (1) is chemically pure and of known composition, (2) has minimal dark toxicity, (3) has preferential uptake

and/or retention by tissues of interest, (4) has rapid excretion leading to low systemic toxicity, (5) has high quantum yield for the generation of singlet oxygen (<sup>1</sup>O<sub>2</sub>), and (6) has a strong absorbance with a high extinction coefficient in the 600–900 nm range where penetration of light into tissue is maximal [8].

We have prepared new photosensitizers, the 21,23-core-modified porphyrins, that possess physical and photophysical properties that are desirable for PDT [9–11]. These molecules are prepared via flexible synthetic schemes that allow the photosensitizers to be tailored for specific applications. The substitution of the heavy atoms S or Se for the core nitrogen atoms of natural porphyrins provides unique physicochemical properties. The core-modified porphyrins do not bind metals due to the larger atomic sizes of S or Se in the 21- and 23-positions [9]. More importantly, a red-shift in light absorption from 630 to 690 nm occurs. These compounds have low dark toxicity as evidenced in earlier experiments where skin photosensitivity was minimal in a murine model, following exposure to a disulfonated core-modified porphyrin and light [9]. Our previous studies of core-modified porphyrins in vitro demonstrated that 5-phenyl-10,15-bis(4-carboxylatomethoxyphenyl)-20-(2-thienyl)-21,23-dithiaporphyrin (**IY69**) showed the greatest potential as a photosensitizer [12].

\* Corresponding author. Present address: Department of Chemistry & Biochemistry, South Dakota State University, Brookings, SD 57007, United States. Tel.: +1 605 688 6905; fax: +1 605 688 6364.

E-mail address: Youngjae.You@sdstate.edu (Y. You).

Photodynamic responses are highly dynamic processes and experimental factors impact biological results both *in vitro* and *in vivo*. We report our initial biological studies *in vitro* for PDT with **IY69** varying several experimental variables: cell line, concentration of the photosensitizer, fluence of light, and time. To examine the pathway of cell death, we determined the induction of apoptosis after PDT with **IY69**. We find that the phototoxicity and the extent of apoptotic cell death using **IY69** as a photosensitizer are significantly affected by the time for which cultured cells are incubated with **IY69** and the concentration of **IY69**.

## 2. Materials and methods

### 2.1. Chemicals and reagents

The detailed synthesis of compound **IY69** appears in an earlier report [12]. Stock solutions of compound **IY69** were prepared in DMSO at  $2 \times 10^{-3}$  M. Serial dilutions were made in sterile doubly distilled water for addition to culture medium. Solvents and reagents were used as received from Sigma–Aldrich Chemical Co. (St. Louis, MO) unless otherwise noted. The Cell Death Detection ELISA<sup>PLUS</sup> assay kit for the detection of apoptosis was purchased from Roche Diagnostics GmbH (Penzberg, Germany). Cell culture medium and antibiotics were purchased from GIBCO (Grand Island, NY). Fetal bovine serum (FBS) was obtained from Atlanta Biologicals (Atlanta, GA).

### 2.2. Cells and culture conditions

The cell lines used for these studies were the R3230AC rat mammary adenocarcinoma cell line and the human breast tumor cell line MCF-7. The cells were maintained in passage culture on 60 mm diameter polystyrene dishes (Becton Dickinson, Franklin Lakes, NJ) in 3.0 mL of minimum essential medium,  $\alpha$ -MEM for the R3230AC cells and Dulbecco's modified essential medium (DMEM) for the MCF-7 cells, supplemented with 10% FBS, 50 U/mL penicillin G, 50  $\mu$ g/mL streptomycin, and 1.0  $\mu$ g/mL Fungizone (complete medium). Only cells from passages 1 to 10 were used for experiments and cells from passages 1 to 4, stored at  $-86$  °C, were used to initiate cultures. Cultures were maintained at 37 °C in a 5% CO<sub>2</sub> humidified atmosphere (Forma Scientific, Marietta, OH). Passage was accomplished by removing the culture medium, adding a 1.0 mL solution containing 0.25% trypsin, incubating at 37 °C for 2–5 min to remove the cells from the surface followed by seeding new culture dishes with an appropriate number of cells in 3.0 mL of medium. Cell counts were performed using a particle counter (model ZM, Coulter Electronics, Hialeah, FL). Cell doubling times were approximately 20 h for the R3230AC cells and approximately 29 h for the MCF-7 cells.

### 2.3. Determination of intracellular accumulation

The amount of intracellular dye was determined using the fluorescence emission of compound **IY69** at 720 nm. Cultured R3230AC or MCF-7 cells were seeded on the inner wells of 96-well plates in the appropriate medium at cell densities ranging from 2 to  $3 \times 10^4$  cells/well and incubated for 24 h. Cells were attached at this point as confirmed by microscopic evaluation. Compound **IY69** was added at  $5 \times 10^{-6}$  M and incubated with the cell monolayer for selected periods from 1 to 24 h. The medium was removed, cells were washed twice with 0.9% NaCl and 0.2 mL of 25% Scintigest<sup>TM</sup> were added to the monolayer and incubated for 1 h at 37 °C. The fluorescence in the cell digests was determined using the multi-well fluorescence plate reader. Excitation at 440 nm produced a peak emission at 720 nm which was used to determine intracellular concentration of **IY69**. Cell numbers were determined as above and the intracellular accumulation of **IY69** was calculated from a fluorescence standard curve generated from known concentrations of **IY69** dissolved in Scintigest<sup>TM</sup>. The cellular concentrations of **IY69** are expressed as femtomole/cell.

### 2.4. Determination of dark- and phototoxicity (MTT assay)

Cytotoxicity (dark- or phototoxicity) was determined by MTT assay [13]. Briefly, cells ( $1.0$ – $1.2 \times 10^4$  cells for R3230AC;  $5$ – $7 \times 10^3$  cells for MCF-7 cells) in 190  $\mu$ L complete medium were plated on the inner wells of 96 well plates. Following incubation of cultured R32320AC or MCF-7 cells with various concentrations of **IY69** for 24 h, the medium was removed, cells were washed twice with 0.2 mL of 0.9% NaCl, and 0.2 mL/well of medium minus FBS and phenol red (clear medium) was added. The plates, with lids removed, were positioned on a orbital shaker (LabLine, Melrose Park, IL) and exposed for various time (less than 1 h) to broadband visible light (350–750 nm) delivered at  $1.4$  mW cm<sup>-2</sup> from a filtered 750 W halogen source defocused to encompass the whole 96 well plate. The culture plates were gently orbited on the shaker in order to ensure uniform illumination of all of the wells on the plate. The clear medium was then removed, 0.2 mL of fresh complete medium was added and cultures were incubated at 37 °C for various times up to 24 h in the dark. To determine dark-toxicity, cell monolayers were also maintained in the dark undergoing the same medium changes and dye additions as those that were irradiated. Cytotoxicity, either dark- or photo-toxicity, was determined using the MTT assay 24 h after the irradiation and expressed as the percent of controls, cells exposed to neither porphyrins nor light.

### 2.5. Cell counting with a particle counter

To determine cell number with or without irradiation, cells were detached with  $1 \times$  trypsin–EDTA and an aliquot of 0.2 mL trypsin solution was added to each well. The

plates were incubated at 37 °C until the cells lifted from the surface (approximately 5 min). Cell counts were performed using a particle counter (Model ZM, Coulter Electronics, Hialeah, FL, USA).

### 2.6. Photodynamic treatment and determination of apoptotic cell death and number of cells

Apoptotic cell death was determined by measuring the DNA fragments (nucleosomes) using the Cell Death Detection ELISA<sup>PLUS</sup> kit and the details followed the instructional manual (Roche Diagnostics, Cat. No. 11 920 685 001) [14]. Cell numbers were determined with the Coulter counter as described above. R3230AC cells were plated on the inner wells of 96 multi-well tissue culture plates at a concentration of  $5 \times 10^3$  cells per well in 190  $\mu\text{L}$  complete medium and incubated for 24 h. Various concentrations of **IY69**,  $5 \times 10^{-8}$ – $4 \times 10^{-6}$  M, were added to the monolayers and incubated for 4 or 24 h at 37 °C in the dark. Following the incubation periods the medium containing **IY69** was removed, 200  $\mu\text{L}$  of clear medium was added to the wells and cells were irradiated as described in the section for measurement of phototoxicity. Clear medium was replaced with 200  $\mu\text{L}$  complete medium, the cells were incubated additionally for 2 h. Cells were counted with a particle counter to determine the number of live cells. To determine apoptotic cell death, cells were lysed and placed into the wells of a streptavidin-coated 96 well plate. By adding a mixture of anti-histone–biotin and anti-DNA–peroxidase, mono- and oligonucleosomes were captured forming sandwich immunocomplexes. Absorbances at 405 and 490 nm were measured after adding ABTS [2,2'-azinodi-(3-ethylbenzthiazoline sulfonate)] substrate. The difference of absorbances (ABS) per  $10^4$  cells was calculated for the unit of nucleosomal production

$$\text{Unit of nucleosomal production} \\ = \text{ABS}[405\text{--}490 \text{ nm}]/10^4 \text{ cells}$$

### 2.7. Statistical analysis

Statistical analyses were performed using the Student's *t*-test. For all tests, *P*-value of less than 0.05 was considered to be a statistically significant difference.

## 3. Results and discussion

### 3.1. Time dependent intracellular accumulation into cultured R3230AC or MCF-7 cells

Cultured R3230AC cells were exposed to  $5 \times 10^{-6}$  M **IY69** for various times. Such a high concentration was employed due to the low intrinsic fluorescence of **IY69** ( $\phi_F = 0.009$ ) [12]. The intracellular concentration of **IY69** reached a plateau after 6–7 h (Fig. 1). Longer incubation times gave no significant increase in cellular accumulation.

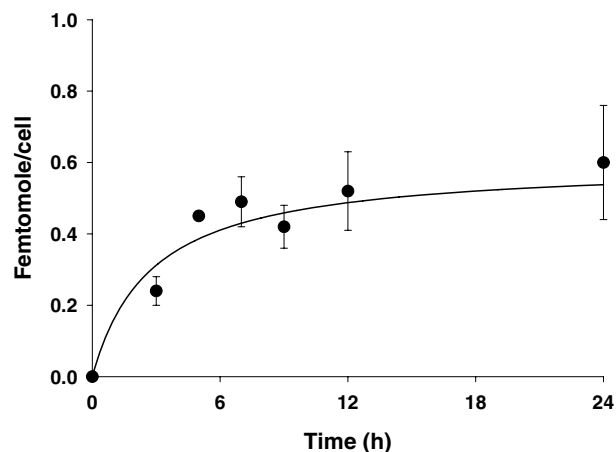


Fig. 1. Time course of intracellular accumulation of **IY69**. Cultured R3230AC cells were incubated with  $5 \times 10^{-6}$  M of **IY69** for various times and the intracellular concentration of **IY69** was determined from its fluorescence. Cell culture conditions, fluorescence determination and calculation of intracellular dye content are detailed in Section 2. Each data point represents the intracellular concentration of **IY69**, expressed as femtomole/cell, determined in 3 separate experiments performed in duplicate, error bars are the SEM.

### 3.2. Dark- and phototoxicity towards cultured R3230AC or MCF-7 cells

No dark toxicity was observed upon incubation of either R3230AC or MCF-7 cells with up to  $1 \times 10^{-6}$  M **IY69** for 24-h as shown in Fig. 2. However, both cell lines showed significant phototoxicity upon irradiation following exposure to **IY69** at concentrations between  $1 \times 10^{-7}$  M and  $1 \times 10^{-6}$  M. Comparable concentrations of **IY69** were more phototoxic toward R3230AC cells than toward MCF-7 cells, which is consistent with the lower intracellular accumulation of **IY69** in the MCF-7 cells (data not shown). However, we cannot exclude other possibilities including a lower level of caspase-3 in MCF-7 cells [15] since at lower concentrations of **IY69** ( $<3 \times 10^{-7}$  M), apoptosis appears to be an important mechanism of cell death as described below in Section 3.6. It has been demonstrated that MCF-7c3 cells, which express more caspase-3 than MCF-7v cells, are more sensitive to apoptotic cell death with the photosensitizer Pc4 than MCF-7v cells although the overall efficacy either in vitro or in vivo is not related to caspase-3 levels in MCF-7 cells [16,17].

### 3.3. Porphyrin and light dose dependency of phototoxicity in cultured R3230AC cells

The data displayed in Fig. 3 demonstrate that phototoxicity towards cultured R3230AC was both porphyrin and light-dose dependent. It appears that the minimum doses required to achieve 40% phototoxicity are  $1 \times 10^{-7}$  M **IY69** combined with at least  $3.75 \text{ J/cm}^2$  of broad band white light delivered at  $1.4 \text{ mW/cm}^2$ . Although **IY69** does not absorb the whole range of broad-band light, its absorption is expected to be proportional to the total fluence of

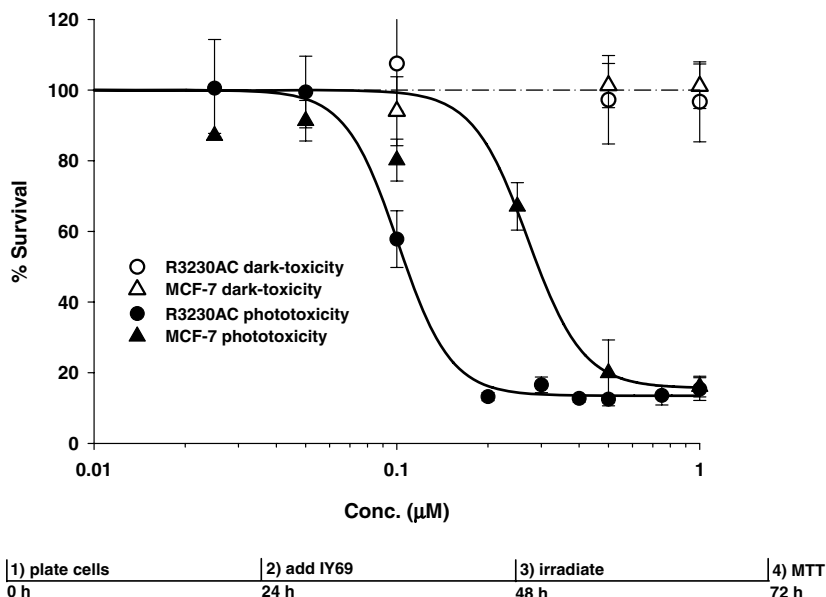


Fig. 2. Dark- and phototoxicity of compound **IY69** towards cultured R3230AC cells (closed symbols) and MCF-7 cells (open symbols). Cell culture and irradiation conditions are detailed in Section 2. Each data point represents the mean of at least 3 separate experiments performed in duplicate, bars are the SEM. Data are expressed as the percent of viable cells compared to control cells (cells not exposed to compound **IY69** or light).

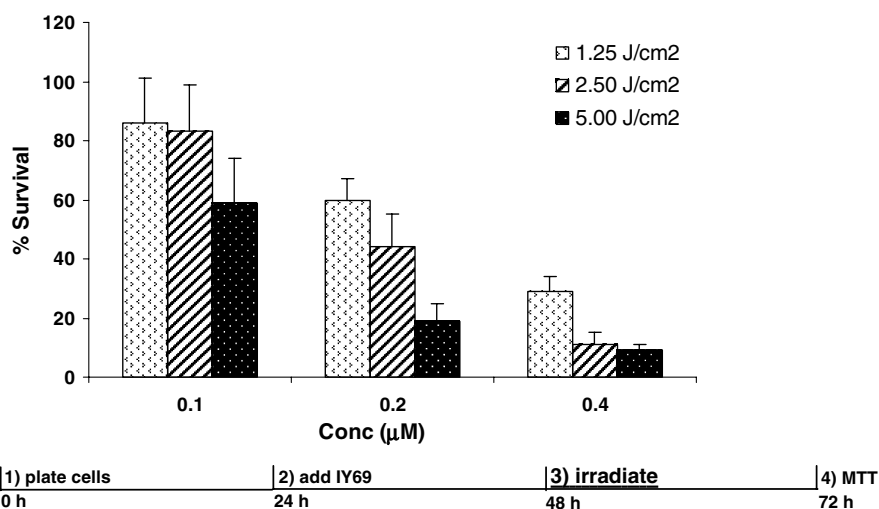


Fig. 3. Porphyrin and light dose related phototoxicity towards cultured R3230AC cells. Cell culture, irradiation conditions and viability determinations using MTT are detailed in Section 2. Each data point represents the mean of at least 3 separate experiments performed in duplicate, bars are the SEM. Data are expressed as the percent of toxicity compared to control cells (cells not exposed to compound **IY69** or light).

the light. The data also show that a relationship between porphyrin dose and total fluence exists. For example, increasing the porphyrin dose allows for a concomitant decrease in the total amount of light delivered to achieve the same level of phototoxicity.

### 3.4. Effects of time after irradiation on phototoxicity towards cultured R3230AC cells

The data displayed in Fig. 4 represent the phototoxicity toward R3230AC cells at various times after the irradiation with **IY69**. Cell counts were determined at different times, 1, 6, 12, and 24 h after irradiation and data are reported

as the ratio of the number of live cells in treated samples to the number of live cells in controls. The data demonstrate that the cell number was significantly decreased by 6 h after irradiation, compared to the number of control cells, for compound **IY69** at  $1 \times 10^{-7}$  M or greater concentration. **IY69** concentrations higher than  $2 \times 10^{-7}$  M plus light continued to elicit a significantly greater decrease in cell viability over the whole 24 h period. Concentrations less than  $5 \times 10^{-8}$  M **IY69** imposed little or no significant phototoxicity until 24 h after irradiation.

Interestingly enough, at  $1 \times 10^{-7}$  M **IY69** cell number was constant up to 12 h after irradiation. To keep the cell number constant up to 12 h, there were two possibilities.

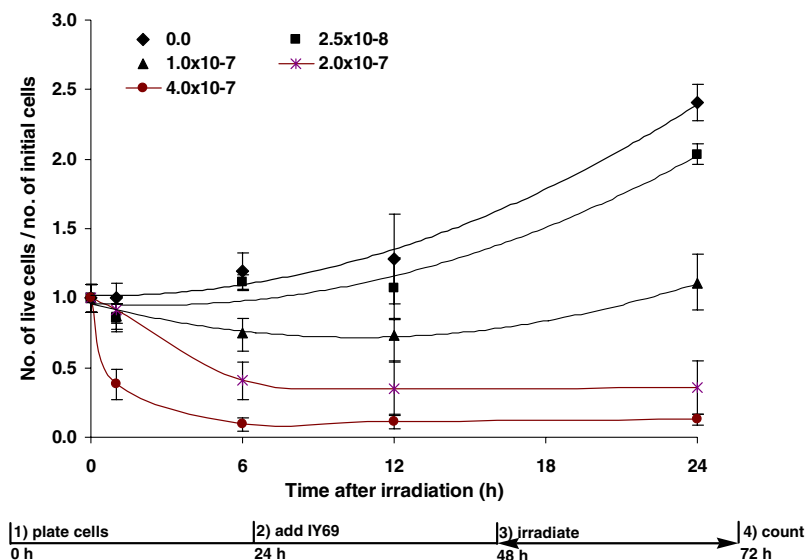


Fig. 4. Time course of R3230AC phototoxicity after irradiation of monolayers exposed to compound **IY69**. Cell culture and irradiation conditions are detailed in Section 2. Each data point represents the mean of at least 2 separate experiments performed in triplicate, bars are the SEM. Data are expressed as ratios of cell numbers counted at various times after irradiation with compound **IY69** at concentrations ranging from 0 to  $4 \times 10^{-7}$  M.

First, the initial cells did not proliferate without cell death, i.e. cytostatic effect. Secondly, some cells died but the other cells doubled quickly to compensate the number of dead cells. Gibson et al. reported cytostatic effect of photodynamic therapy of 0.05 mM  $\delta$ -ALA with  $30 \text{ mJ/cm}^{-2}$  irradiation [18]. It is not clear which is the case in this experiment. However, cell number slightly increased at 24 h although overall phototoxicity at 24 h was 54% compared to the control, which means cells regain their proliferate capacity. It will be interesting to observe the long term effects on phototoxicity and more detailed mechanistic study which will elucidate dynamic cellular responses to low dose photodynamic treatment with **IY69**.

### 3.5. Effect of incubation time of cells with **IY69** before irradiation on phototoxicity

Phototoxicity was determined for cultured R3230AC cells incubated with compound **IY69** for various times prior to irradiation. The cells were exposed to **IY69** for 1, 3, 5, 7, 9, 12, 18, or 24 h, then, irradiated with  $5 \text{ J/cm}^{-2}$  of broad-band light. Phototoxicity was determined 24 h after the irradiation. The data displayed in Fig. 5 show that the longer cells are incubated with compound **IY69**, the more effective the subsequent light treatment becomes. At higher concentrations, e.g. ( $1 \times 10^{-6}$  M), significant levels of cytotoxicity can be reached at much shorter incubation

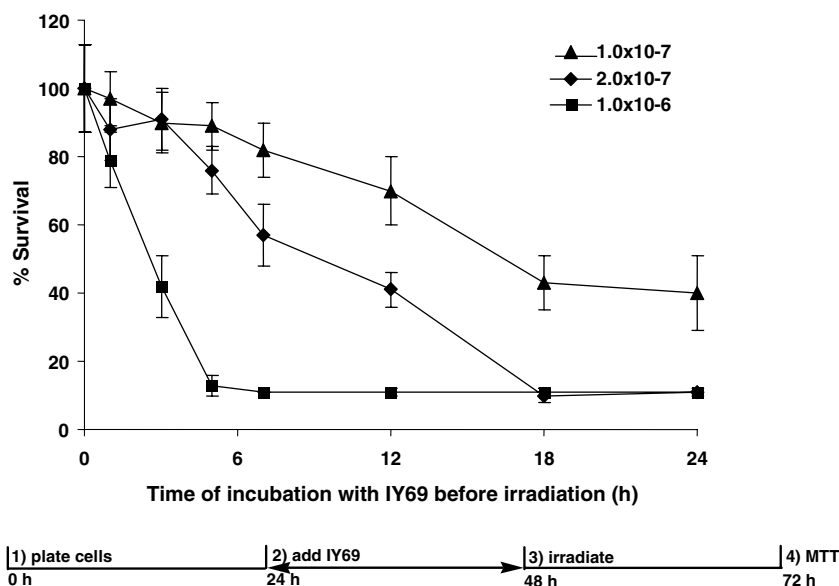


Fig. 5. Effect of time of exposure of cultured R3230AC cells to compound **IY69** prior to irradiation on phototoxicity. Cell culture, irradiation conditions and cytotoxicity determinations using MTT are detailed in Section 2. Each data point represents the mean of at least 3 separate experiments performed in duplicate, bars are the SEM. Data are expressed as the percent of control cell cytotoxicity (cells not exposed to compound **IY69** or light).

intervals, within 6 h with incubation time-dependent manner. If we assume that the kinetics of uptake at these concentrations, 1, 2, or  $10 \times 10^7$  M, is similar to that at  $5 \times 10^{-6}$  M (Fig. 1), the time-dependent phototoxicity of **IY69** up to 6 h is consistent with the time-dependent concentration of **IY69** in cells.

Incubation time-dependency of phototoxicity was also absorbed after 6 h in cells treated with 2 or  $1 \times 10^{-7}$  M **IY69**. The difference of phototoxicity at 6 and 24 h with  $1 \times 10^{-7}$  and  $2 \times 10^{-7}$  M cannot be explained by the difference in concentration because the amounts of **IY69** at 6 and 24 h are expected to be similar. In our fluorescence microscopic study, the distributions of fluorescence from **IY69** in cells at 4 and 24 h after addition were different: most of fluorescence seemed evenly distributed throughout cells after 4 h (data not shown). On the other hand, localized bright spots of the fluorescence were absorbed in cells at 24-h after the addition of **IY69** without staining nuclei [12]. The sites of localization of photosensitizers are the sites of initial photodamage by singlet oxygen generated

by photodynamic therapy: it has been generally believed that life time of singlet oxygen is short, 0.03–0.18  $\mu$ s in vivo, thus diffusion distance of singlet oxygen is very limited [19]. Thus, we presume that the localization of **IY69** in specific sites inside cells with longer incubation make the photosensitizer more efficient in expressing phototoxicity.

### 3.6. Effect of incubation time of cells with **IY69** on induction of apoptotic cell death

We determined the degree of photo-induced apoptosis after 4- or 24-h incubation of cultured R3230AC cells with various concentrations of **IY69** as well as the number of cells in parallel for phototoxicity. Apoptotic cell death was measured using the Cell Death Detection ELISA<sup>PLUS</sup> kit provided by Roche diagnostics. This kit determines the presence of mono- and oligonucleosomes in the cytosol of cell lysates as one representative indication of the DNA degradation following the induction of apoptosis [20,21]. The data displayed in Fig. 6 reveal the importance of both

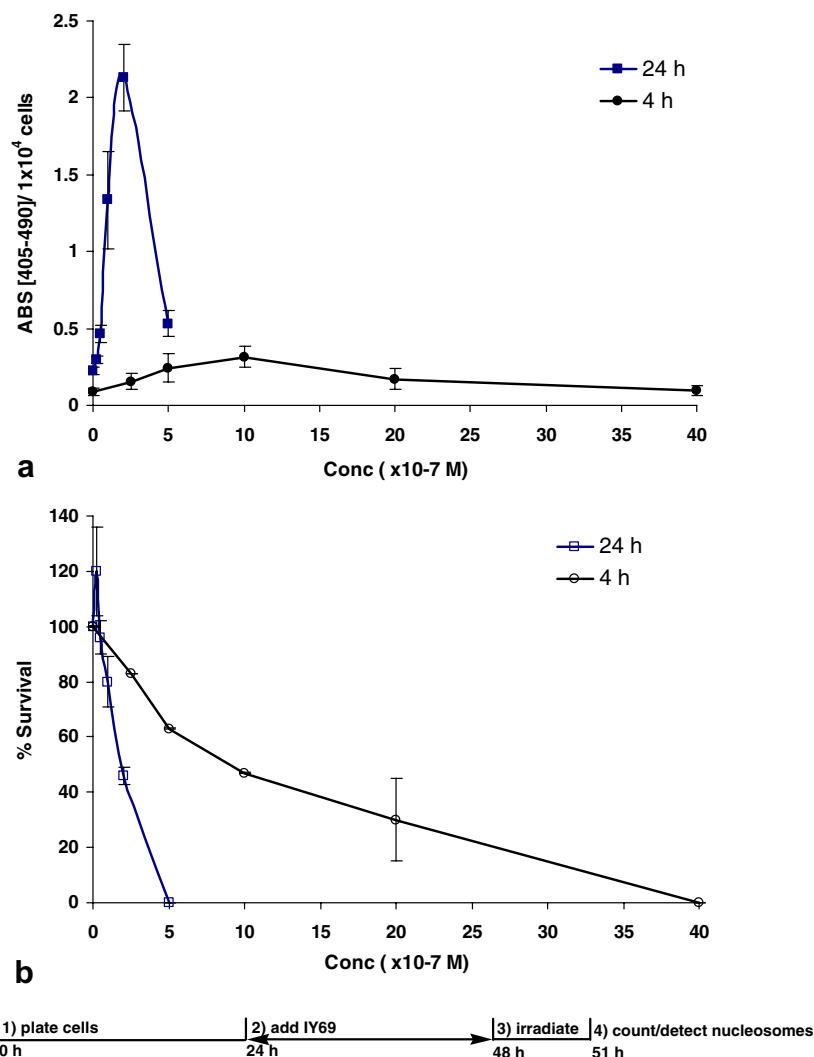


Fig. 6. Determination of cell number and apoptosis. Cell culture and irradiation conditions are detailed in Section 2. Each data point represents the mean of at least 3 separate experiments performed in duplicate, bars are the SEM.

the concentration of **IY69** and the time of exposure of cultured R3230AC cells to **IY69** on both phototoxicity and induction of apoptosis.

The level of phototoxicity was dependent on the concentration of **IY69** for cells exposed for either 4 h or for 24 h to the photosensitizer (Fig. 6a). For any given concentration, 24-h exposure to the photosensitizer gave increased phototoxicity relative to a 4-h exposure. As an example, exposure to  $5 \times 10^{-7}$  M **IY69** and light gave nearly 100% phototoxicity while a 4-h exposure gave around 40% phototoxicity.

The production of mono- and oligonucleosomes due to the induction of apoptosis was affected by the concentration of **IY69** (Fig. 6b). However, the effect did not solely depend on the concentration of **IY69**. There were optimal concentrations for the maximal production of nucleosomes for both 4 and 24-h exposure conditions, 0.3 and 2.1 units (ABS[405–490]/ $1 \times 10^4$  cells) at  $1 \times 10^{-6}$  and  $2 \times 10^{-7}$  M **IY69**, respectively. At higher concentrations above the optimal conditions, the production of nucleosomes decreased (Fig. 6b). The production of nucleosomes reached minimal points, 0.53 and 0.094 units at high concentrations,  $5 \times 10^{-7}$  and  $4 \times 10^{-6}$  M **IY69** for 4 and 24-exposures. The concentration of photosensitizers in cells was reported as one of the main factors influencing pathway of cell death after PDT [22–26]. It was consistent in PDT with **IY69** that the mode of cell death shifted pathway from pro-apoptotic to pro-necrotic as concentration of a photosensitizer increased.

The other interesting result was the effect of exposure time of **IY69** to the cells on induction of apoptosis. Overall, PDT with 24-h exposure of **IY69** produced more nucleosomes than that with 4-h exposure. At the optimal conditions, longer exposure of **IY69** to R3230AC cells at lower concentration,  $2 \times 10^{-7}$  M for 24 h, produced the more nucleosomes than shorter exposure at higher concentration,  $1 \times 10^{-6}$  M for 4 h. The production of nucleosomes at  $2 \times 10^{-7}$  M with 24-h exposure was seven times the amount of nucleosomes at  $1 \times 10^{-6}$  M with 4-h exposure: 2.1 vs. 0.3 units. Considering this result with the intracellular localization 24 h after addition of **IY69** [12], it is likely that the sites of localization of **IY69** with 24-h exposure were important organelles for apoptosis. This hypothesis is supported by previous reports where the sites of localization of photosensitizers in cells were primary photodamage sites, consequently important in determining cell death pathway in PDT: apoptosis or necrosis [6,22,27–31].

#### 4. Conclusion

The new photosensitizer, **IY69**, was phototoxic towards both cultured R3230AC rat mammary tumor cells and MCF-7 human breast cancer cells. The phototoxicity toward R3230AC cells exposed to **IY69** and light was dependent on various experimental conditions such as concentration of the **IY69**, total fluence of light, the length of time post irradiation, and exposure time of **IY69** to cultured R3230AC cells. Especially, the time of exposure of

**IY69** to R3230AC cells was a main factor for cellular concentration, localization, and cell death mechanism after irradiation. We are thus under process to find molecular mechanistic and pharmacokinetic profiles of photodamage and localization in PDT with **IY69**.

#### Acknowledgement

This research was supported by the Department of Defense [Breast Cancer Research Program] under award number W81XWH-04-1-0500. Views and opinions of, and endorsements by the author(s) do not reflect those of the US Army or the Department of Defense.

#### References

- [1] H. Kato, Photodynamic therapy for lung cancer – a review of 19 years' experience, *J. Photochem. Photobiol. B* 42 (1998) 96–99.
- [2] D. Ost, Photodynamic therapy in lung cancer. A review, *Methods Mol. Med.* 75 (2003) 507–526.
- [3] R.L. Prosst, H.C. Wolfsen, J. Gahlen, Photodynamic therapy for esophageal diseases: a clinical update, *Endoscopy* 35 (2003) 1059–1068.
- [4] F. Guillemin, X. Feintrenie, D. Lignon, [Photodynamic therapy of bronchogenic cancer], *Rev. Pneumol. Clin.* 48 (1992) 111–114.
- [5] D.E.B.W.G. Love, Photodynamic therapy comes of age, *IDrugs* 3 (2000) 1487–1508.
- [6] T.J. Dougherty, C.J. Gomer, B.W. Henderson, G. Jori, D. Kessel, M. Korbelik, J. Moan, Q. Peng, Photodynamic therapy, *J. Natl. Cancer Inst.* 90 (1998) 889–905.
- [7] M.R. Detty, S.L. Gibson, S.J. Wagner, Current clinical and preclinical photosensitizers for use in photodynamic therapy, *J. Med. Chem.* 47 (2004) 3897–3915.
- [8] M.R. Detty, Photosensitizers for the photodynamic therapy of cancer and other diseases, *Expert Opin. Ther. Pat.* 11 (2001) 1849–1860.
- [9] C.E. Stilts, M.I. Nelen, D.G. Hilmey, S.R. Davies, S.O. Gollnick, A.R. Oseroff, S.L. Gibson, R. Hilf, M.R. Detty, Water-soluble, core-modified porphyrins as novel, longer-wavelength-absorbing sensitizers for photodynamic therapy, *J. Med. Chem.* 43 (2000) 2403–2410.
- [10] D.G. Hilmey, M. Abe, M.I. Nelen, C.E. Stilts, G.A. Baker, S.N. Baker, F.V. Bright, S.R. Davies, S.O. Gollnick, A.R. Oseroff, S.L. Gibson, R. Hilf, M.R. Detty, Water-soluble, core-modified porphyrins as novel, longer-wavelength-absorbing sensitizers for photodynamic therapy. II. Effects of core heteroatoms and meso-substituents on biological activity, *J. Med. Chem.* 45 (2002) 449–461.
- [11] Y. You, S.L. Gibson, R. Hilf, S.R. Davies, A.R. Oseroff, I. Roy, T.Y. Ohulchanskyy, E.J. Bergey, M.R. Detty, Water soluble, core-modified porphyrins. 3. Synthesis, photophysical properties, and in vitro studies of photosensitization, uptake, and localization with carboxylic acid-substituted derivatives, *J. Med. Chem.* 46 (2003) 3734–3747.
- [12] Y. You, S.L. Gibson, R. Hilf, T.Y. Ohulchanskyy, M.R. Detty, Core-modified porphyrins. Part 4: Steric effects on photophysical and biological properties in vitro, *Bioorg. Med. Chem.* 13 (2005) 2235–2251.
- [13] T. Mosmann, Rapid colorimetric assay for cellular growth and survival: application to proliferation and cytotoxicity assays, *J. Immunol. Methods* 65 (1983) 55–63.
- [14] H. Dika Nguea, B. Rihn, D. Mahon, J.L. Bernard, A. De Reydellet, A. Le Faou, Effects of various man-made mineral fibers on cell apoptosis and viability, *Arch. Toxikol.* 79 (2005) 487–492.
- [15] F. Essmann, I.H. Engels, G. Totzke, K. Schulze-Osthoff, R.U. Janicke, Apoptosis resistance of MCF-7 breast carcinoma cells to ionizing radiation is independent of p53 and cell cycle control but caused by the lack of caspase-3 and a caffeine-inhibitable event, *Cancer Res.* 64 (2004) 7065–7072.

- [16] L.Y. Xue, S.M. Chiu, N.L. Oleinick, Photodynamic therapy-induced death of MCF-7 human breast cancer cells: a role for caspase-3 in the late steps of apoptosis but not for the critical lethal event, *Exp. Cell Res.* 263 (2001) 145–155.
- [17] C.M. Whitacre, T.H. Satoh, L. Xue, N.H. Gordon, N.L. Oleinick, Photodynamic therapy of human breast cancer xenografts lacking caspase-3, *Cancer Lett.* 179 (2002) 43–49.
- [18] S.L. Gibson, J.J. Havens, M.L. Nguyen, R. Hilf, Delta-aminolaevulinic acid-induced photodynamic therapy inhibits protoporphyrin IX biosynthesis and reduces subsequent treatment efficacy in vitro, *Brit. J. Cancer* 80 (1999) 998–1004.
- [19] M. Niedre, M.S. Patterson, B.C. Wilson, Direct near-infrared luminescence detection of singlet oxygen generated by photodynamic therapy in cells in vitro and tissues in vivo, *Photochem. Photobiol.* 75 (2002) 382–391.
- [20] O.S. Frankfurt, A. Krishan, Apoptosis enzyme-linked immunosorbent assay distinguishes anticancer drugs from toxic chemicals and predicts drug synergism, *Chem. Biol. Interact.* 145 (2003) 89–99.
- [21] O.S. Frankfurt, A. Krishan, Enzyme-linked immunosorbent assay (ELISA) for the specific detection of apoptotic cells and its application to rapid drug screening, *J. Immunol. Methods* 253 (2001) 133–144.
- [22] N.L. Oleinick, R.L. Morris, I. Belichenko, The role of apoptosis in response to photodynamic therapy: what, where, why, and how, *Photochem. Photobiol. Sci.* 1 (2002) 1–21.
- [23] F. Rancan, A. Wiehe, M. Nobel, M.O. Senge, S.A. Omari, F. Bohm, M. John, B. Roder, Influence of substitutions on asymmetric dihydroxychlorins with regard to intracellular uptake, subcellular localization and photosensitization of Jurkat cells, *J. Photochem. Photobiol. B* 78 (2005) 17–28.
- [24] S. Gupta, B.S. Dwarakanath, K. Muralidhar, V. Jain, Role of apoptosis in photodynamic sensitivity of human tumour cell lines, *Indian J. Exp. Biol.* 41 (2003) 33–40.
- [25] J.F. Tremblay, S. Dussault, G. Viau, F. Gad, M. Boushira, R. Bissonnette, Photodynamic therapy with toluidine blue in Jurkat cells: cytotoxicity, subcellular localization and apoptosis induction, *Photochem. Photobiol. Sci.* 1 (2002) 852–856.
- [26] M. Dellinger, Apoptosis or necrosis following Photofrin photosensitization: influence of the incubation protocol, *Photochem. Photobiol.* 64 (1996) 182–187.
- [27] D. Kessel, Y. Luo, Photodynamic therapy: a mitochondrial inducer of apoptosis, *Cell Death Differ.* 6 (1999) 28–35.
- [28] M.H. Teiten, S. Marchal, M.A. D'Hallewin, F. Guillemin, L. Bezdetsnaya, Primary photodamage sites and mitochondrial events after Foscan photosensitization of MCF-7 human breast cancer cells, *Photochem. Photobiol.* 78 (2003) 9–14.
- [29] C. Fabris, G. Valduga, G. Miotto, L. Borsetto, G. Jori, S. Garbisa, E. Reddi, Photosensitization with zinc (II) phthalocyanine as a switch in the decision between apoptosis and necrosis, *Cancer Res.* 61 (2001) 7495–7500.
- [30] D. Kessel, Y. Luo, Intracellular sites of photodamage as a factor in apoptotic cell death, *J. Porphy. Phthalocya.* 5 (2001) 181–184.
- [31] D. Kessel, Y. Luo, Y. Deng, C.K. Chang, The role of subcellular localization in initiation of apoptosis by photodynamic therapy, *Photochem. Photobiol.* 65 (1997) 422–426.